

Two-Neutron Quasiparticle States Observed in ^{236}U with the (d, p) Reaction*

K. Katori,* A. M. Friedman, and J. R. Erskine
Argonne National Laboratory, Argonne, Illinois 60439
 (Received 12 April 1973)

Energy levels in the nucleus ^{236}U have been studied with the $^{235}\text{U}(d, p)^{236}\text{U}$ reaction at bombarding energies from 12 to 16 MeV. The reaction products were analyzed with a split-pole magnetic spectrograph. The strongest transitions are those that lead to two-neutron quasiparticle states. Four rotational bands built upon the $\frac{7}{2}^- [743] \pm \frac{1}{2}^+ [631]$ and $\frac{7}{2}^- [743] \pm \frac{5}{2}^+ [622]$ configurations were identified. The bandheads for the $K^\pi = 1^-, 4^-, 3^-,$ and 6^- bands are found to be at 970, 1054, 1192, and 1472 keV, respectively. The single-particle cross sections were extracted from the measured cross sections to the members in the rotational bands that involve the $\frac{1}{2}^+ [631]$ orbital. Disagreement with calculated single-particle cross sections was found similar to the corresponding disagreement for cross sections extracted from the data on population of this orbital by transfer reactions on even-even targets. Measured energy splittings in both ^{236}U and ^{234}U are compared with calculated values.

I. INTRODUCTION

Investigation of pure two-quasiparticle states in strongly deformed even-even nuclei is important to an understanding of low-lying collective states from the microscopic point of view. Two-quasiparticle states in an even-even nucleus can be selectively populated through stripping and pickup reactions such as (d, p) , $(^3\text{He}, d)$, $(^4\text{He}, t)$, (d, t) and $(^3\text{He}, ^4\text{He})$ on an odd-mass target nucleus. A two-quasiparticle excitation represents the motion of two unpaired protons or neutrons that couple their spin projections Ω_1 and Ω_2 either parallel or antiparallel to form states with $K_\geq = |\Omega_1 \pm \Omega_2|$. Although many two-quasiparticle states are expected to lie above 1 MeV in even-even actinide nuclei, only a limited number of these are populated by a single-neutron transfer reaction. Specifically, the (d, p) process can populate only configurations of the type $(F, F+m)$, where F denotes the Nilsson orbital of the neutron in the ground state of the target and $(F+m)$ denotes the single-particle orbital of the transferred neutron in the excited state. The primary aim of this study is to identify two-neutron quasiparticle states in even-even actinide nuclei.

The second aim of this study is to investigate the $T=1$ components of the effective residual interaction in strongly deformed nuclei. Measured energy splittings between K_+ and K_- states can be compared with the calculated values, as can the energy shifts extracted from the unperturbed two-quasiparticle level energies estimated from the energies of one-quasiparticle states in neighboring odd- A nuclei. Since the matrix elements of the residual interaction for identical particles have only $T=1$ components, the residual interaction has fewer parameters than in the general case.

Pure two-quasiparticle states with pure configurations in even-even nuclei are therefore favorable cases for studies (1) of the need for finite-range forces and (2) of the consistency between the force and range parameters in the residual interaction in deformed nuclei and the corresponding parameters in spherical nuclei.

The third aim is to investigate the high-angular-momentum-transfer transitions to two-quasiparticle states. In his study of sub-Coulomb transfer reactions on a number of actinide targets, Erskine¹ found a large discrepancy between the measured and the calculated cross sections for $J \geq \frac{7}{2}$ transitions to one-quasiparticle final states. The question is whether a similar discrepancy exists also for similar transitions to two-quasiparticle states. In the case of two-quasiparticle final states, the orbitals of the transferred neutrons are the same as were involved in one of the reactions studied by Erskine, but the use of an odd- A target introduces the additional complexity that several values of l transfer contribute to the cross section. Under certain assumptions, the differential cross sections to members in the same band can be decomposed into a sum of single-particle cross sections for the individual values of l . These extracted cross sections can then be compared with calculated single-particle cross sections. The discrepancy between the measured and calculated cross sections above the Coulomb barrier have been investigated experimentally at bombarding energies of 12, 14, and 16 MeV.

The reasons for choosing ^{236}U for the present study were that it lies in the region of heavy nonspherical nuclei with well developed rotational bands and that the single-particle states in adjacent odd- A nuclei are well known. The neighboring odd-mass nuclei ^{235}U and ^{237}U have been ex-

tensively studied by Braid *et al.*,² von Egidy, Elze, and Huizenga,³ and Rickey, Jurney, and Britt.⁴ These investigations showed that the spectra of intrinsic excitations are well described by the Nilsson model. Low-lying states in ^{236}U have also been investigated through studies of (n, γ) reactions,^{5,6} (p, t) reactions,⁷ and (d, d') inelastic scattering⁸ at excitation energies up to 1.3 MeV. The states excited in these reactions were mainly collective states such as those in the ground-state band, in the β and γ vibrational bands, and in the octupole vibrational bands.

In ^{234}U , Bjornholm, Dubois, and Elbek⁹ have identified four two-quasiparticle states through (d, p) and (d, t) reactions. In ^{236}U , similar two-quasiparticle states are expected. Discussion focuses on two-neutron quasiparticle states formed by coupling a $\frac{7}{2}^-$ [743] orbital for the first neutron in the target to $\frac{5}{2}^+$ [622] and $\frac{1}{2}^+$ [631] orbitals for the second neutron.

II. EXPERIMENTAL PROCEDURE AND RESULTS

The 12-MeV deuteron beam was provided by the Argonne FN tandem accelerator. The ^{235}U target was prepared with an electromagnetic isotope separator in the Argonne Chemistry Division. The beam from the separator deposited about $100 \mu\text{g}/\text{cm}^2$ of uranium directly onto a carbon backing, which had a thickness of about $40 \mu\text{g}/\text{cm}^2$.

Protons were detected in photographic emulsions placed in the local plane of an Enge split-pole magnetic spectrograph.¹⁰ Plates were scanned with a computer-controlled automatic nuclear-

emulsion scanner.¹¹ The accuracy of these results was checked occasionally by hand scanning.

The absolute cross sections were measured relative to the elastic scattering cross section of the deuteron beam on the target. Elastically scattered deuterons were recorded by a silicon monitor detector at 90° . At this angle, the ratio to Rutherford scattering for 12-MeV deuterons is known experimentally¹² to be 0.70 ± 0.03 . The beam energy was determined and the solid angle of the monitor was calibrated by means of elastic scattering measurements with the spectrograph.

A typical spectrum is shown in Fig. 1. The over-all energy-resolution width is about 10 keV. Proton spectra were taken at 90° , 105° , 120° , and 135° and were analyzed with the peak-fitting program AUTOFIT.¹³ Energy levels were observed up to 2.7 MeV excitation in ^{236}U . These are tabulated in Table I. The ground-state band was not observed; an upper limit of $1 \mu\text{b}/\text{sr}$ can be set on the cross sections to its members.

Since the ground state was not observed, excitation energies were determined by measuring the absolute Q value for the various levels in ^{236}U and subtracting these from 4.320 MeV, the ground-state Q value derived from Kane's measured value⁵ (6.545 ± 0.002 MeV) for the neutron separation energy in ^{236}U . In this way, excitation energies of 671 ± 5 , 729 ± 5 , 1023 ± 5 , and 1039 ± 5 keV were obtained directly from our data. Recently Boyno *et al.*⁸ studied the $^{236}\text{U}(d, d')^{236}\text{U}$ reaction and reported levels at 686, 746, 1037, and 1060 keV. Also the (n, γ) studies⁶ find levels at 687.73, 744.33, and 1053.06 keV. It is probable although

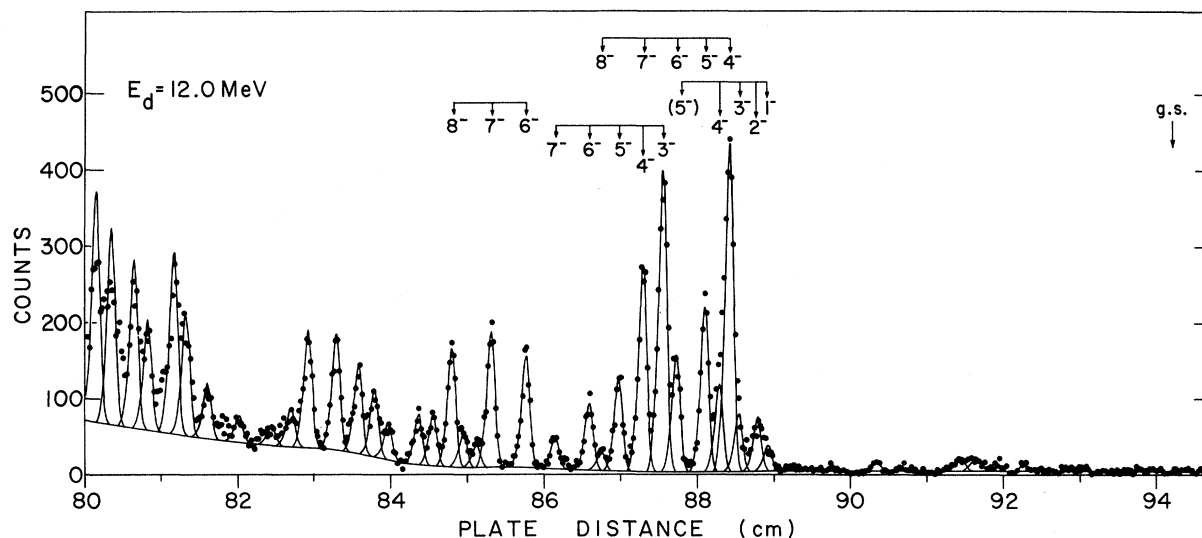


FIG. 1. Typical proton spectrum for the $^{235}\text{U}(d, p)^{236}\text{U}$ reaction at 90° . The levels assigned in the present work are indicated.

not certain that the (d, p) reaction reported above excites the same levels as were excited in the (d, d') and (n, γ) reactions. An unknown systematic error in the method we used to obtain our excitation energies would account for the approximately 15-keV lower energy we measure. Therefore, in the rest of this paper, all our measured excitation energies have been increased by 15 keV to bring them into agreement with the (n, γ) and (d, d') results. Figure 2 compares the ^{236}U energy levels observed in the various reactions. In Table I, all levels assigned to any particular band are grouped together.

III. CALCULATION OF DIFFERENTIAL CROSS SECTIONS

The differential cross section for a stripping or pickup process on a nonspherical target nucleus can be expressed in terms of the Nilsson wave functions and intrinsic single-particle transfer cross sections as obtained from a distorted-wave Born-approximation (DWBA) calculation.¹⁴ For the case of no Coriolis mixing between states, the cross section for a reaction to a final state in an even-even or odd-odd residual nucleus can be

TABLE I. The ^{236}U levels observed with the $^{235}\text{U}(d, p)^{236}\text{U}$ reaction in the present work.

Configuration ^a	K^π	I^π	Excitation energy ^b (keV)	Differential cross section			
				90° ($\mu\text{b}/\text{sr}$)	105° ($\mu\text{b}/\text{sr}$)	120° ($\mu\text{b}/\text{sr}$)	135° ($\mu\text{b}/\text{sr}$)
$F, F+2$	1^-	(0^+)	686.4±2.5	1.0±0.2	1.5±0.3	2.2±0.3	1.7±0.2
		(3^-)	744.4±1.1	2.1±0.2	2.3±0.3	2.2±0.3	1.4±0.2
		1^-	969.7±1.9	5.8±0.9	4.4±0.6	2.7±0.6	2.1±0.4
		2^-	991.5±1.9	12.1±1.2	5.8±0.7	5.2±0.7	4.7±0.5
		3^-	1038.1±3.4	12.9±1.5	14.1±1.3	16.4±1.5	8.1±0.8
$F, F+1$	4^-	4^-	1072.3±2.5	19.6±1.8	14.4±1.3	12.7±1.2	12.0±1.1
		5^-	(1164.0)	(12.5)	(13.1)	(10.8)	(10.3)
		4^-	1053.9±1.4	71.9±2.9	69.5±2.2	53.1±2.2	46.6±1.6
		5^-	1104.4±1.4	36.5±1.9	35.4±1.3	31.5±1.3	23.0±0.9
		6^-	1164.0±2.6	26.2±1.5 ^c	28.5±1.3 ^c	26.2±1.3 ^c	23.8±1.3 ^c
$F, F+1$	3^-	7^-	(1232.2)	(6.9)	(6.0)	(6.4)	(5.0)
		8^-	1320.0±3.5	4.2±0.8	3.6±0.6	4.4±0.6	4.5±0.8
		3^-	1191.6±1.0	66.3±2.3	66.5±1.8	52.4±1.7	48.3±1.8
		4^-	1232.2±1.0	45.5±1.9 ^c	46.5±1.5 ^c	38.9±1.4 ^c	35.8±1.5 ^c
		5^-	1282.2±1.0	20.1±1.3	23.3±1.1	20.3±1.1	17.6±1.1
$F, F+2$	6^-	6^-	1342.8±1.0	14.9±1.2	18.4±1.0	16.4±1.0	11.0±2.6
		7^-	1413.3±1.9	7.5±1.0	10.1±1.2	7.6±0.8	6.2±0.7
		6^-	1471.7±1.0	24.7±1.0	31.7±2.0	24.0±1.3	22.8±1.2
		7^-	1541.8±1.3	29.9±0.9	39.3±2.0	33.5±1.2	35.0±1.2
		8^-	1621.8±1.2	26.2±0.9	38.9±2.1	26.1±1.1	29.3±1.1
			1575.4±1.8	5.1±0.5	7.8±1.1	3.8±0.5	3.9±0.5
			1600.8±1.0	7.6±0.6	16.2±1.6	7.7±0.8	6.9±0.7
			1658.1±2.3	11.2±0.6	22.8±1.6	9.8±0.7	9.6±0.7
			1689.6±1.7	11.1±0.6	17.4±1.4	10.1±0.7	11.8±0.8
			1748.0±2.6	8.1±1.1	5.8±3.1	6.8±3.8	4.8±2.4
			1775.9±2.2	14.8±1.4	20.1±5.1	20.6±5.9	19.4±3.9
			1811.3±1.3	19.8±1.6	19.1±5.0	22.0±5.8	17.3±3.6
			1854.8±2.0	25.4±1.7	29.6±5.9	31.4±6.8	29.2±4.7
			1912.0±1.6	26.0±1.8	27.4±5.7	22.9±6.0	16.9±3.7
			1946.8±2.0	8.7±1.1	10.0±3.8	9.0±4.2	9.6±2.8
	2052.6±2.1	5.6±4.6	2.0±2.1	2.6±2.6	7.3±2.6		
	2114.2±2.7	11.6±6.3	9.1±3.7	6.1±3.4	6.0±2.4		
	2155.1±1.5	25.2±9.1	21.3±5.6	23.5±6.8	15.7±4.0		
	2176.9±1.8	35.5±11.1	36.1±7.3	31.8±8.3	23.4±4.7		
	2200.6±3.4	12.5±7.3	11.6±4.8	15.5±6.8	8.8±3.1		
	2234.0±0.4	22.9±8.8	23.7±6.8	24.9±6.9	20.9±4.2		
	2260.4±1.0	33.3±10.3	35.6±6.7	26.5±6.8	24.9±4.6		

^a In the configuration column, F stands for $\frac{7}{2}^- [743]$, $F+1$ for $\frac{1}{2}^+ [631]$, and $F+2$ for $\frac{5}{2}^+ [622]$.

^b These energies are not our measured energies but have been shifted 15 keV to bring them into agreement with the (n, γ) and (d, d') results. See text for details.

^c Sum of the cross sections for a doublet.

written

$$\frac{d\sigma_{\alpha}^{I_f}}{d\sigma} = \sum_j P_{\alpha} \langle I_i j K_i K_f | I_f K_f \rangle^2 C_{j\alpha}^2 \theta_j^{DW}(\vartheta), \quad (1)$$

where $d\sigma_{\alpha}^{I_f}/d\Omega$ is the differential cross section to a member of rotational band α , the $C_{j\alpha}^2$ are the expansion coefficients of the Nilsson wave function of the orbit into which the transferred neutron is captured, P_{α} is the value of the pairing emptiness factor U_{α}^2 for the capturing orbit in the special case of a (d, p) reaction, θ_j^{DW} is the single-particle differential cross section, j is the total angular momentum of the transferred neutron, I_i and I_f are the target and final-state spins, K_i and K_f are the values of angular momentum projection along the nuclear symmetry axis for the initial and final states, and $K = |K_i - K_f|$.

In general for an even-even or odd-odd residual nucleus, several values of j may contribute to the population of a given final state I_f, K_f . The contribution of several j values to each cross section makes the intensity patterns for the rotational bands less characteristic than for the case of an odd- A residual nucleus. On the other hand, levels of the same rotational band are populated with intensities that vary slowly with I_f , and this facilitates the separation of levels into rotational bands.

The single-particle differential cross sections θ_j^{DW} were calculated with the program DWUCK.¹⁵ The angular distributions measured by Macefield and Middleton¹⁶ are well described by the same parameters as were used in the work on even-even

targets.² These parameters as well as the other sets of optical parameters tested are listed in Table II. The cross sections were found to be insensitive to reasonable variations in the optical-model parameters. A normalization factor of 1.65 was applied to the zero-range DWBA calculation to obtain the (d, p) cross section. The Nilsson wave functions are computed with the parameter $\mu = 0.45$, $\kappa = 0.05$, and $\beta = 0.25$. For the emptiness factors we used the values obtained² in the analysis of the energy levels of ²³⁵U, namely $U_{\alpha}^2 = 0.5$ for the $\frac{1}{2}^+$ [631] orbital of the transferred neutron and 0.75 for the $\frac{5}{2}^+$ [622] orbital.

Differential cross sections were computed with the program BANDMIX.¹⁸ The effects of Coriolis band mixing on the differential cross sections were taken into account in the calculation. The matrix elements used were calculated from the Nilsson wave functions. The differential cross sections for the populations of the members of a rotational band depend strongly on the Nilsson wave function of the orbital entered by the transferred neutron. Thus, the relative cross sections give a characteristic signature which is an important aid to assigning the two-quasiparticle states that make up the band.

IV. ASSIGNMENT OF LEVELS

The procedure used to make spin and configuration assignments of the observed levels is roughly sketched below. Further details are included in the discussions of the individual assignments. The steps taken are as follows:

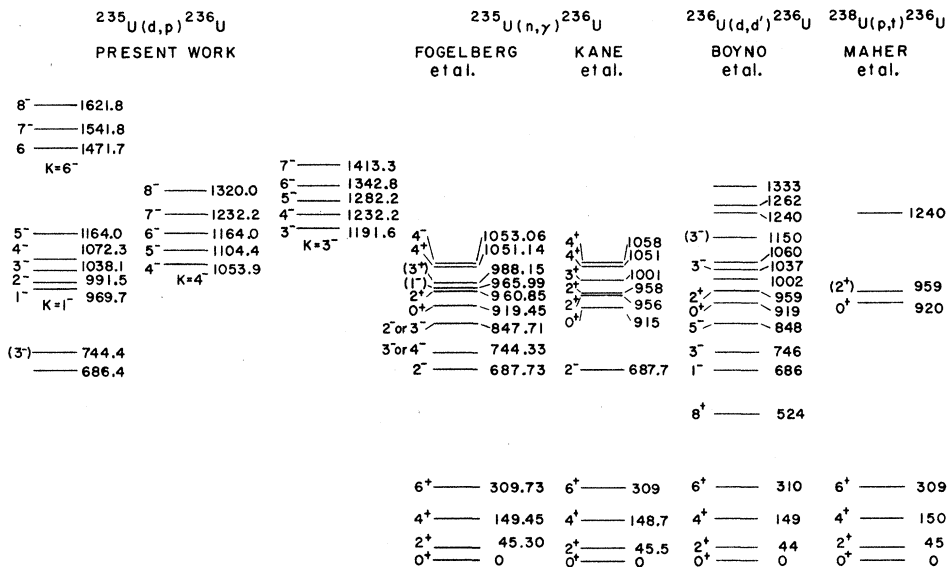


FIG. 2. Energy-level schemes of ²³⁸U as deduced from (d, p) , (n, γ) , (d, d') , and (p, t) experiments.

(1) The experimental energies of the two-quasiparticle states are compared with the energies estimated, without taking account of the residual interaction, from the energies of one-quasiparticle states in adjacent odd-mass nuclei.

(2) The relative intensities of levels in the band are calculated, and the resulting characteristic signatures are compared with the observed levels.

(3) The $I(I+1)$ rule in energy is applied in each band.

(4) The experimental cross sections are summed over all levels belonging to a given band and the result is compared with the corresponding calculated sum.

(5) Steps (1)–(4) are repeated at other angles in order to confirm the assignment.

(6) The spins and parities of low-lying levels in ^{238}Np are known.¹⁹ These have been identified as levels formed by coupling a $\frac{5}{2}^+[642]$ proton orbital to the $\frac{1}{2}^+[631]$ and $\frac{5}{2}^+[622]$ neutron orbitals. The experimental ratios of cross sections measured in the $^{235}\text{U}(d,p)^{236}\text{U}$ reaction to those to corresponding members of the respective bands in the $^{237}\text{Np}(d,p)^{238}\text{Np}$ reaction are compared with the calculated ratios in order to confirm the spin assignments.

Only four low-lying bands are expected to be observed in the $^{235}\text{U}(d,p)^{236}\text{U}$ reaction. The $K^\pi = 3^-$ and 4^- bands are formed by coupling a $\frac{7}{2}^-[743]$ orbital to a $\frac{1}{2}^+[631]$ orbital, and the $K^\pi = 1^-$ and 6^- bands are from coupling a $\frac{7}{2}^-[743]$ orbital to a $\frac{5}{2}^+[622]$ orbital. On the basis of energy systematics, these are expected at $E_x = 950\text{--}1500$ keV.

Effects from collective states such as β and γ quadrupole-vibrational states are expected to be small, since the low-lying two-quasiparticle excitations in ^{236}U are negative-parity states, and

TABLE II. Parameters for the optical-model potential

$$U(r) = -V(1 + \exp X)^{-1} - iW(1 + \exp X')^{-1},$$

where

$$X = (r - r_0 A^{1/3})/a \text{ and } X' = (r - r'_0 A^{1/3})/a'.$$

Potential I is taken from Ref. 2. Potential III is taken from Ref. 17.

Potential No.	Particle	V_0 (MeV)	r_0 (fm)	a (fm)	r'_0 (fm)	W (MeV)	r'_0 (fm)	a' (fm)	λ
I	d	60.0	1.5	0.6	1.5	15.0	1.5	0.6	
	p	57.0	1.3	0.5	1.3	8.0	1.3	0.5	
	n		1.25	0.65					25
II ^a	d		1.35	0.71					25
	n								
III	d	109.9	1.063	1.038	1.25	9.8	1.501	0.728	
	p	57	1.3	0.5	1.30	8.0	1.30	0.5	
	n		1.25	0.65					25

^a The optical-potential parameters used for d and p in potential II are the same as those in potential I.

the β and γ vibrational states have positive parity. Pure octupole-vibrational states, which have negative parity, are expected to be weakly populated. But two-quasiparticle states may mix with octupole states, and the mixed octupole states might then be observed in a transfer reaction.

A. Levels Resulting from Transitions into the $\frac{1}{2}^+[631]$ Neutron Orbital

On the basis of excitation-energy estimates for two-quasiparticle states, the expected signature, and the $I(I+1)$ rule in energy, the 1054-, 1104-, 1164-, 1232-, and 1320-keV levels are assigned to be members of the $K^\pi = 4^-$ rotational band formed by coupling the $\frac{7}{2}^-[743]$ and $\frac{1}{2}^+[631]$ neutron orbitals. Similarly, the 1192-, 1232-, 1282-, 1343-, and 1413-keV levels are assigned to the $K^\pi = 3^-$ rotational band. Two accidental doublets occur in the spectra. In one, the 7⁻ level in the $K^\pi = 4^-$ band coincides with the 4⁻ level in the $K^\pi = 3^-$ band. In the other, the 6⁻ level in the $K^\pi = 4^-$ band coincides with the 5⁻ level in the $K^\pi = 1^-$ band. These doublets were decomposed by

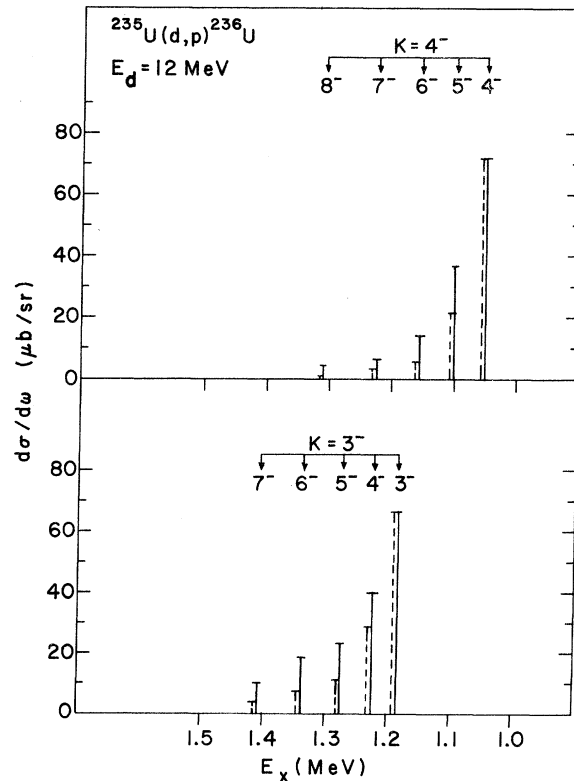


FIG. 3. Comparison of calculated cross sections (dashed bars) and experimental ones (solid bars) for the $K^\pi = 3^-$ and 4^- bands at 90° . The calculated values are normalized at the 3⁻ level in the $K^\pi = 3^-$ band and at the 4⁻ level in the $K^\pi = 4^-$ band.

using the extracted single-particle cross sections in a way which will be discussed in Sec. V A. In Fig. 3, the relative magnitudes of the calculated cross sections within each band are compared with the corresponding experimental cross sections obtained in Sec. II. The calculated differential cross sections are normalized to the 3^- level in the $K^\pi = 3^-$ band and the 4^- level in the $K^\pi = 4^-$ band. Good agreement is obtained. Similar comparisons at 105, 120, and 135° showed similar agreement. On the assumption that energies for the levels in each band follow the $I(I+1)$ rule, the rotational energy parameter A was found to be 5.05 ± 0.17 keV for the $K^\pi = 3^-$ band and 5.02 ± 0.12 keV for the $K^\pi = 4^-$ band. Five levels of each band were used for a least-squares fit to the formula.

Of course, Coriolis mixing between 3^- and 4^- bands should be taken into account in calculating the differential cross section. The effect of mixing is illustrated in Table III, which shows the results calculated with and without mixing for the particular case of the $I_f = 4$ level. The largest change in cross section was the 10% found for a level in the 4^- band; the change was only 1.7 and 5.3% for the 4^- level in the 4^- and 3^- bands, respectively. The energy shift was ≤ 9 keV even for the states of highest spin; at the band head it was only 1 keV, as seen in Table III.

An independent way to assign these levels is to

TABLE III. Spectroscopic factors S_j , calculated with and without Coriolis band mixing, for the $I_f = 4^-$ level in the $K^\pi = 4^-$ and 3^- bands of the $\{\frac{3}{2}^- [743] \pm \frac{1}{2}^+ [631]\}$ configurations. The expression without band mixing is

$$S_{j\alpha} = \frac{2I_i + 1}{2I_f + 1} \langle I_i K_i j K | I_f K_f \rangle^2 C_{j\alpha}^2 U_\alpha^2,$$

where the chosen value of the emptiness factor for the $\frac{1}{2}^+ [631]$ orbital is $U_\alpha^2 = 0.5$. The excitation energies and differential cross sections at the band head are given in the last two rows.

j	$K^\pi = 4^-$ band		$K^\pi = 3^-$ band	
	Mixed	Unmixed	Mixed	Unmixed
$\frac{1}{2}$	0.053 01	0.056 27	0.010 29	0.007 03
$\frac{3}{2}$	0.103 41	0.093 76	0.037 22	0.046 88
$\frac{5}{2}$	0.003 37	0.004 00	0.005 13	0.004 50
$\frac{7}{2}$	0.008 80	0.007 23	0.012 90	0.014 47
$\frac{9}{2}$	0.003 24	0.004 33	0.014 63	0.013 54
$\frac{11}{2}$	0.001 37	0.001 03	0.004 27	0.004 61
$\frac{13}{2}$	0.000 01	0.000 02	0.000 11	0.000 10
E_x (keV)	1053.0	1054.0	1233.4	1232.4
$\frac{d\sigma}{d\Omega}$ ($\mu\text{b/sr}$)	65.5	64.4	21.9	23.1

compare them with similar ^{238}Np levels populated in the $^{237}\text{Np}(d, p)^{238}\text{Np}$ reaction at the same bombarding energy. The spin and parity for low-lying levels in ^{238}Np are well established, and these levels are known¹⁹ to be members of the $K^\pi = 2^+$ and 3^+ bands formed by coupling the $\frac{5}{2}^+ [642]$ proton orbital to a $\frac{1}{2}^+ [631]$ neutron orbital. According to Eq. (1) for the differential cross section, all the factors in the sum over j are the same as in the ^{236}U case, except for the Clebsch-Gordan coefficient. The transferred orbital $\frac{1}{2}^+ [631]$ is the same but the spin of the target is different. In another investigation reported elsewhere,²⁰ proton spectra were measured at 90 and 120° with the $^{237}\text{Np}(d, p)^{238}\text{Np}$ reaction at $E_d = 12$ MeV and were analyzed in the same way as in the $^{235}\text{U}(d, p)^{236}\text{U}$ reaction. The ratios of the cross sections for these two reactions are plotted in Fig. 4, where the measured ratios are shown as solid circles and the theoretical ratios from Eq. (1) are shown as open circles. The experimental ratios have been normalized by setting them equal to the theoretical ratios at the band heads. Excellent agreement is obtained. The spin and parity assignments in the 3^- and 4^- bands are confirmed by this independent method.

The measured and calculated cross sections were next summed over all observed final levels I_f within a band. These summed cross sections $(\frac{d\sigma_\alpha}{d\Omega})_\Sigma$ are defined as

$$\left(\frac{d\sigma_\alpha}{d\Omega}\right)_\Sigma = \sum_{I_f} \frac{d\sigma_\alpha^{I_f}}{d\Omega} = \sum_{I_f} \sum_j U_\alpha^2 \langle I_i j K_i K | I_f K_f \rangle^2 C_{j\alpha}^2 \theta_j^{\text{DW}}. \quad (2)$$

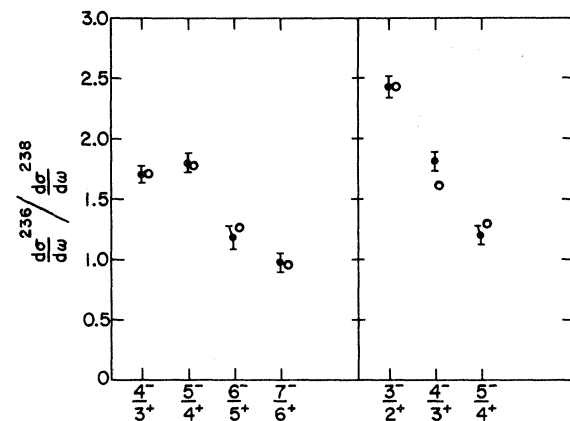


FIG. 4. Ratios of the differential cross sections $d\sigma^{236}/d\Omega$ for the $^{235}\text{U}(d, p)^{236}\text{U}$ reaction to the differential cross sections $d\sigma^{238}/d\Omega$ for the $^{237}\text{Np}(d, p)^{238}\text{Np}$ reaction to corresponding members of the respective bands. The cross sections measured at 120° to the beam are shown as solid circles with error bars. Open circles are the ratios calculated with the DWBA. Experimental ratios are normalized to the calculated ratios at the band heads.

The measured and calculated summed cross sections for the $K^\pi = 4^-, 3^-, 1^-$, and 6^- bands are tabulated in Table IV. The pairing emptiness factor U_α^2 for each band is taken to be unity in this calculation. For the set of θ_j^{DW} , the optical-potential parameters for potential I (Table II) are used.

At each angle the largest summed cross section in the measurement corresponds to the $K^\pi = 3^-$ band, and the next largest one corresponds to the $K^\pi = 4^-$ band. The ratio R of the experimental summed cross section to the calculated one is given in the table for each angle. The average ratio \bar{R} for all angles for $K^\pi = 3^-$ band is the same within statistical error as that for $K^\pi = 4^-$ band. This supports the level assignment for $K^\pi = 3^-$ and $K^\pi = 4^-$ bands, since the transferred neutron enters the same neutron orbit for both the $K^\pi = 3^-$ and 4^- bands.

The angular distributions also give some information for spin assignments. The 3^- and 4^- levels in the 3^- and 4^- bands involve an $l=0$ component of the single-particle cross section. For $l \geq 5$, an $l=0$ transition is not allowed. Therefore, forward-peaked angular distributions should indicate the presence of an $l=0$ component in the transition and suggest 3^- and 4^- states in the $K^\pi = 3^-$ and 4^- bands. In the observed angular distributions (Table I), the 90° cross sections for the levels to which we have assigned 3^- and 4^- are higher than those for the 5^- and 6^- levels. This is consistent with our spin assignments.

These measurements also can give information about the purity of the two-quasiparticle configuration of the $K^\pi = 4^-$ and 3^- bands. The rotational energy parameter A for these bands (about 5.0 keV) is consistent with that of pure two-quasiparticle states in nearby actinide nuclei (see Sec. VB). In addition, the ratios of the cross sections for populating these bands to the cross sections for populating the bands built on the $\frac{1}{2}^+[631]$ neutron orbital in ^{238}Np is the same for both the $K^\pi = 3^-$ and 4^- bands. This could only be true if either the mixing for both bands was the same in both ^{238}Np and ^{236}U or if they both were unmixed in either nuclei. Also the fact that the average ratio \bar{R} of the measured cross sections to the calculated ones is the same for both bands (see Table IV) again indicates that either both states are mixed to the same degree or that they are both pure. For these reasons we believe the $K^\pi = 4^-$ and 3^- bands in ^{236}U to be pure two-quasiparticle states.

B. Levels Resulting from Transitions into the $\frac{5}{2}^+[622]$ Neutron Orbital

On the basis of estimated excitation energies for two-quasiparticle states, the calculated signature, and the $I(I+1)$ rule in energy, the 1472-, 1542-, and 1622-keV levels are assigned to be members of the $K^\pi = 6^-$ rotational band formed by coupling the $\frac{7}{2}^-[743]$ and $\frac{5}{2}^+[622]$ neutron orbitals in ^{236}U ; and the 970-, 992-, 1038-, 1072-, and

TABLE IV. Summary of the summed cross sections for the $K^\pi = 4^-, 3^-, 1^-$, and 6^- bands at the four indicated angles. The last column represents the purity of the two-quasiparticle component of the band. In this calculation the 4^- band is taken to consist entirely of two-quasiparticle states.

K	Range of I^π	θ_{lab} (deg)	Summed cross section ($\mu\text{b}/\text{sr}$)		R	\bar{R}	$\frac{\bar{R}^a}{U_\alpha^2}$	Purity (%)
			Experiment ^b	Calculated ^c				
4^-	$(4^- - 8^-)$	90	133.1 ± 7.1	183	0.72 ± 0.04	0.83 ± 0.04	1.67 ± 0.08	100
		105	129.9 ± 5.4	158	0.82 ± 0.03			
		120	110.8 ± 5.4	126	0.88 ± 0.04			
		135	92.7 ± 5.0	102	0.91 ± 0.05			
3^-	$(3^- - 7^-)$	90	147.4 ± 7.6	203	0.72 ± 0.04	0.89 ± 0.05	1.79 ± 0.09	107 ± 11
		105	158.8 ± 6.6	175	0.91 ± 0.04			
		120	130.2 ± 5.9	141	0.92 ± 0.04			
		135	117.6 ± 7.4	115	1.02 ± 0.06			
1^-	$(1^- - 5^-)$	90	62.8 ± 5.4	60	1.05 ± 0.09	0.93 ± 0.07	1.24 ± 0.15	74 ± 12
		105	51.7 ± 3.8	58	0.89 ± 0.07			
		120	48.8 ± 3.9	52	0.92 ± 0.07			
		135	37.2 ± 2.8	44	0.85 ± 0.06			
6^-	$(6^- - 8^-)$	90	80.7 ± 2.8	81	0.99 ± 0.03	1.21 ± 0.05	1.62 ± 0.11	97 ± 11
		105	109.8 ± 6.1	80	1.37 ± 0.08			
		120	83.6 ± 3.6	74	1.13 ± 0.05			
		135	87.1 ± 3.5	64	1.36 ± 0.06			

^a The value $U_\alpha^2 = 0.50$ is taken for the $K^\pi = 4^-$ and 3^- bands, $U_\alpha^2 = 0.75$ for $K^\pi = 1^-$ and 6^- .

^b The uncertainty stated is the sum of the uncertainties for the individual members of the band.

^c Potential I is used to calculate the differential cross sections.

1164-keV levels are assigned to the $K^\pi = 1^-$ rotational band. The relative magnitudes of the experimental and calculated cross sections at $\theta_{\text{lab}} = 90^\circ$ are compared in Fig. 5. The calculated cross section is normalized to the 6^- level in the $K^\pi = 6^-$ band and 4^- level in $K^\pi = 1^-$ band. Good agreement is obtained. Similar comparisons with the 105, 120, and 135° data gave similar good agreement.

The rotational-energy parameters A extracted by least-squares fitting are 4.97 ± 0.17 keV for the $K^\pi = 6^-$ band and 6.69 ± 0.34 keV for the $K^\pi = 1^-$ band. The value of the A parameter extracted for the $K^\pi = 6^-$ band is the same as those for the 3^- and 4^- bands (5.02 and 5.05, respectively) within the experimental uncertainty, but the value extracted for the $K^\pi = 1^-$ band is larger. As mentioned at the beginning of Sec. IV, this may be due to the coupling between octupole-vibrational states and/or the negative-parity two-quasiparticle states with low K . The spacing between levels in the $K^\pi = 1^-$ band does not follow the $I(I+1)$ rule exactly. The 2^- and 4^- levels are shifted relative to the 1^- , 3^- , and 5^- levels.

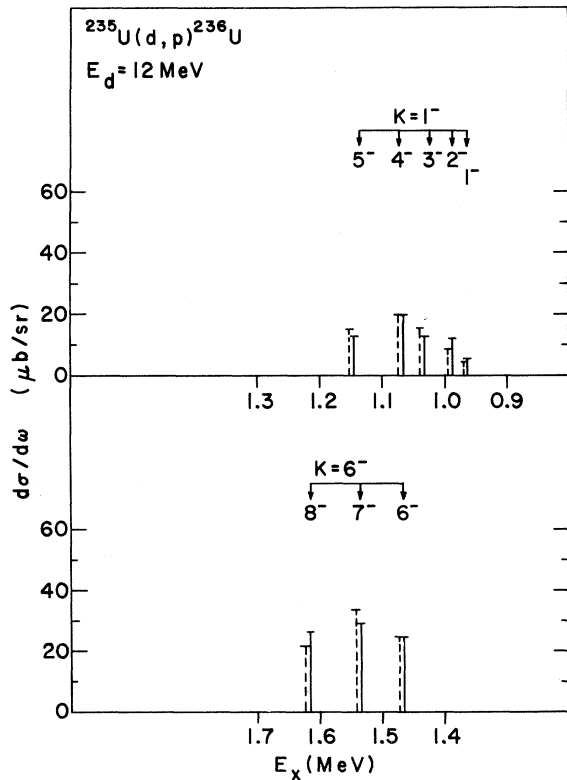


FIG. 5. Comparison of calculated cross sections (dashed bars) and experimental ones (solid bars) for the $K^\pi = 6^-$ and $K^\pi = 1^-$ bands at 90° . The data are normalized at the 6^- level in the $K^\pi = 6^-$ band and at the 4^- level in the $K^\pi = 1^-$ band.

For the $K^\pi = 6^-$ band, as for the $K^\pi = 3^-$ and 4^- bands, an independent way to assign the levels is to compare the yields with those for the corresponding states in the $^{237}\text{Np}(d, p)^{238}\text{Np}$ reaction. The ratios are shown in Fig. 6 along with the corresponding calculated ratios. The fairly good agreement obtained supports the level assignment.

The summed cross sections of all levels in a band are compared in Table IV. The ratio R of experimental summed cross sections to calculated ones is not as constant as for the $K^\pi = 3^-$ and 4^- bands. Hence the ratio R was averaged over all angles to reduce the uncertainties on the experimental data and calculated cross sections. The resulting average ratio \bar{R} for the $K^\pi = 6^-$ band was then compared with one for the $K^\pi = 4^-$ band by calculating the double ratio $\bar{R}(K=4^-)/\bar{R}(K=6^-)$ which should be proportional to $[U(K=4^-)/U(K=6^-)]^2$ because taking the ratio largely cancels the uncertainties in the DWBA calculation. The experimental ratio $\bar{R}(K=4^-)/\bar{R}(K=6^-) = 0.687 \pm 0.033$ agrees quite well with the theoretical ratio $[U(K=4^-)/U(K=6^-)]^2 = 0.50/0.75 = 0.67$ between the predicted values of U^2 for the $\frac{1}{2}^+[631]$ and $\frac{5}{2}^+[622]$ orbitals. This suggests that the $K^\pi = 6^-$ band is a pure two-quasiparticle state, as the $K^\pi = 4^-$ and $K^\pi = 3^-$ bands also are.

In a similar comparison of the summed cross sections to the 4^- and 1^- bands, the double ratio of experimental values was found to be $\bar{R}(K=4^-)/\bar{R}(K=1^-) = 0.898 \pm 0.060$. If the $K^\pi = 1^-$ band were a pure two-quasiparticle state, this double ratio

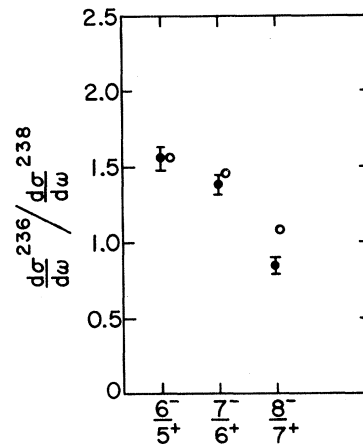


FIG. 6. Ratios of the differential cross sections $d\sigma^{236}/d\Omega$ for the $^{235}\text{U}(d, p)^{236}\text{U}$ reaction to the differential cross sections $d\sigma^{238}/d\Omega$ for the $^{237}\text{Np}(d, p)^{238}\text{Np}$ reaction to corresponding members of the respective bands. The cross sections were measured at $\theta = 120^\circ$. The open circles represent the corresponding ratios calculated with the DWBA and normalized to the experimental ratio for the reactions to the band head.

should be the same as that for the 4^- and 6^- bands; i.e., one should have

$$\begin{aligned} \bar{R}(K=4^-)/\bar{R}(K=1^-) &= \bar{R}(K=4^-)/\bar{R}(K=6^-) \\ &= [U(K=4^-)/U(K=6^-)]^2 = 0.67. \end{aligned}$$

In fact, however, the double ratios are quite different; instead of equal values of \bar{R} for the $K^\pi = 1^-$ and 6^- bands, one finds the ratio $\bar{R}(K=1^-)/\bar{R}(K=6^-) = 0.76$. This suggests that the $K^\pi = 1^-$ band is not a pure two-quasiparticle state.

The purity of the two-quasiparticle configurations is here defined as suggested by Bjornholm, Dubois, and Elbek,⁹ whose basic assumption was that the effect of configuration mixing can be factored out of the differential cross sections for reactions to collective states. Thus they write

$$\left(\frac{d\sigma}{d\Omega}\right)_{\text{mixed}} = P \left(\frac{d\sigma}{d\Omega}\right)_{\text{pure}}$$

where P is the purity of the two-quasiparticle state. (In Ref. 9, P is called the "square of the amplitude.") In the present case of the $K^\pi = 1^-$ band, the purity of the $\{\frac{7}{2}^-[743] \pm \frac{5}{2}^+[622]\}$ configuration is 0.76; the remaining 24% of the amplitude of this configuration is lost to octupole vibrational states and other collective states. This result for $K^\pi = 1^-$ is consistent with the (d, d') experiment,⁸ in which the transition to the 3^- level at 1037 keV was found to be stronger than would be expected from the transition to the 3^- level at 746 keV.

C. Other Levels

Octupole vibrational states are not expected to be strongly populated through the (d, p) reaction, since octupole states are considered to consist of many two-quasiparticle states, no one of which is predominant. The $K^\pi = 0^-$ and 2^- octupole vibrational states are expected to be below 1 MeV in ²³⁶U. The most likely way to excite those states in a (d, p) reaction is through Coriolis coupling to the $K^\pi = 1^-$ states, although intensities may not be large.

The inelastic scattering of deuterons on actinide nuclei has been studied by Elze and Huizenga,²¹ and by Boyno *et al.*⁸ For ²³⁶U, Boyno *et al.*⁸ have tentatively assigned 1^- , 3^- , and 5^- to levels at 686, 746, and 848 keV in the octupole vibrational $K^\pi = 0^-$ band. In the (n, γ) experiment,^{5,6,22} however, the 687.7-keV level is assigned to be 2^- . In recent measurements on electron conversion following thermal-neutron capture,⁶ two possibly additional levels were observed at 744.3 and 847.7 keV and were assigned to be 3^- or 4^- and 2^- or 3^- , respectively.

We observe two levels at 686 and 744 keV and tentatively assign them to be 1^- and 3^- levels in the $K^\pi = 0^-$ octupole vibrational band, but the spins and parities for those levels could not be identified from our results. The 1^- and 3^- assignment is preferred to the 2^- and 3^- assignment for the 686- and 744-keV levels on the ground that that assignment implies a more reasonable moment of inertia. The possibility of a doublet consisting of 1^- ($K^\pi = 0^-$) and 2^- ($K^\pi = 2^-$) levels cannot be excluded.

Many levels have been observed above 1550 keV, but we have not been able to make convincing configuration assignments for them. We have tried to make assignments by first calculating the expected cross sections to two-quasiparticle states that involve the $\frac{1}{2}^+[620]$, $\frac{3}{2}^+[622]$, $\frac{7}{2}^+[613]$, $\frac{1}{2}^-[761]$, and other neutron orbitals. The fact that the observed cross sections are smaller than any calculated ones suggests fragmentation of the levels. The level density above 2-MeV excitation energy is so high that one cannot separate the individual peaks in the observed (d, p) spectrum.

V. DISCUSSION

A. Comparison Between Calculated and Measured Single-Particle Cross Sections

The single-particle cross sections for particular angular momenta were extracted from the measured cross sections for reactions to the observed levels. The extraction procedure used was more complicated than for a transfer reaction on an even-even target, since in our case several l values are involved in the transitions. The basis of the method we used is that for transitions to various members of the same rotational band, the same set of values of $C_{j\alpha}$ and θ_j^{DW} are involved; only the Clebsch-Gordan coefficients change. This can be seen by examining Eq. (1), the formula for the cross section. In this equation, all of the quantities except θ_j^{DW} are known or can reasonably be assumed. Hence this single-particle cross section is regarded as an adjustable parameter to be extracted from the data by use of a matrix method of least-squares analysis (of which a general discussion is given, for example, by Ferguson²³). These extracted single-particle cross sections will be designated ϕ_j to distinguish them from the values computed from distorted-wave theory θ_j^{DW} .

For this purpose, Eq. (1) was rewritten in matrix form as

$$[d\sigma] = U_\alpha^2 [A] \times [B], \quad (3)$$

where the elements of $[d\sigma]$ are the measured cross sections $d\sigma_{\alpha}^f/d\Omega$ for the reactions to the various members of the rotational band, the elements of

[A] are in general a rectangular matrix $A_{j_i j_f}$ $= \langle I_i j_i K_i K | I_f j_f K_f \rangle^2$, and the elements of [B] are $B_j = C_{j\alpha}^2 \phi_j$. The matrix [B] can be found by solving Eq. (3) by standard matrix methods. The assumptions here are (1) that the single-particle cross section for $j = l - \frac{1}{2}$ is equal to that for $j = l + \frac{1}{2}$ and (2) that the expansion coefficients $C_{j\alpha}$ for the deformed single-particle wave function are well described by Nilsson wave functions. If these assumptions are valid, one can then extract the individual single-particle cross sections ϕ_j .

In Fig. 7, the extracted individual single-particle cross section ϕ_l for the $\frac{1}{2}^+[631]$ orbital is shown as a function of transferred angular momentum and is compared with the single-particle cross section θ_l^{DW} calculated in DWBA with three sets of optical parameters designated as potentials I, II, and III and listed in Table II. The optical-model parameters for potentials I and II are the same for protons and deuterons; but for neutrons, potential I has the nuclear-radius parameter $r_0 = 1.25$ fm and the diffuseness parameter $a = 0.65$ fm for a bound state, while potential II has $r_0 = 1.35$ fm and $a = 0.71$ fm. The absolute cross sections calculated with potential II are larger than those for potential I by a factor of 1.9–2.7, but the general trends of the two curves are the same. For potential III, the proton and neutron parameters are the same as for potential I, but the deuteron parameters are different. None of these potentials can reproduce the extracted single-particle cross sections. As seen in Fig. 7, the extracted cross section at $l=0$ is considerably below the DWBA curves, but at $l=4$ and 6, the extracted cross sections are much above the calculated curves. Only at $l=2$ does the extracted cross section come close to the DWBA cross section. The same procedure was repeated with the data obtained at other angles. The results are similar to the results at 90° for both $K^\pi = 3^-$ and $K^\pi = 4^-$ bands.

The diminution of the $l=0$ transition and the enhancement of higher l transitions for the $\frac{1}{2}^+[631]$ orbital were also observed in the (d, p) and (d, t) reactions on the even-even targets ^{232}Th and ^{238}U below the Coulomb barrier.¹ Furthermore, the same trend has been found for the $\frac{1}{2}^+[631]$ orbital with the $^{237}\text{Np}(d, p)^{238}\text{Np}$, $^{237}\text{Np}(d, t)^{238}\text{Np}$, and $^{243}\text{Am}(d, t)^{242}\text{Am}$ reactions at 12 MeV bombarding energy.²⁰

For the $\frac{5}{2}^+[622]$ orbital, the single-particle cross sections (Fig. 8) were extracted in the same way. An enhancement for $l=4$ and 6 transitions is observed at 12 MeV as before, but the difference is not as striking as for the $\frac{1}{2}^+[631]$ orbital.

In order to check how the $C_{j\alpha}$ factors depend on the deformation parameters β , the $C_{j\alpha}$ factors for $\beta = 0.30$ were calculated. The change in cross sec-

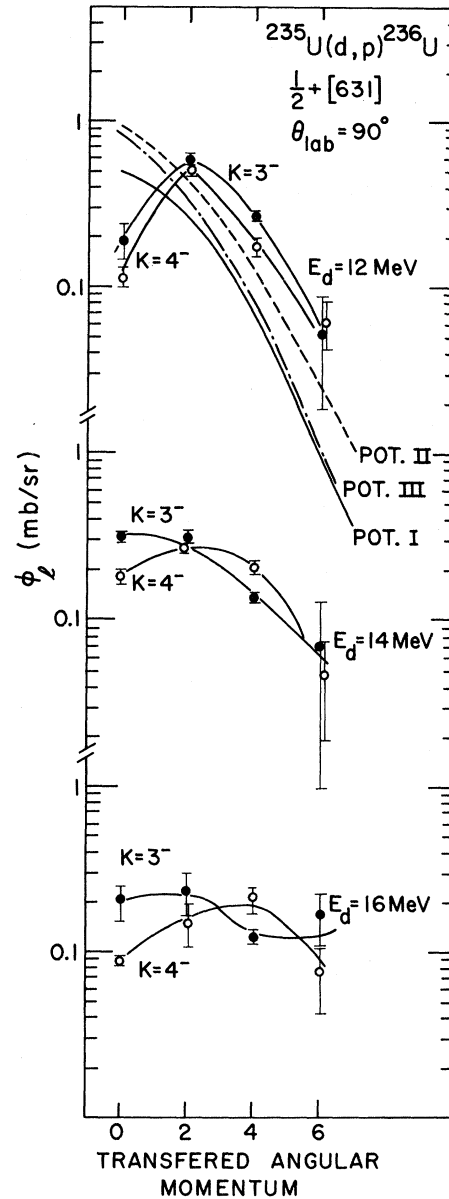


FIG. 7. Single-particle cross sections ϕ_l for (d, p) transitions to members of the $K^\pi = 3^-$ band (filled circles) and 4^- band (open circles) in ^{236}U . The experimental cross sections from which these values of ϕ_l were extracted were measured at bombarding energies of 12, 14, and 16 MeV—which are at and above the Coulomb barrier. Spectroscopic factors of the $\frac{1}{2}^+[631]$ orbital were calculated for the deformation parameters $\beta = 0.25$, $\kappa = 0.05$, and $\mu = 0.45$. Coriolis mixing between the $K^\pi = 3^-$ and 4^- bands is taken into account. The experimental values at $E_d = 12$ MeV are compared with the DW curves calculated with potentials I, II, and III. The solid curves through experimental points are drawn only to guide the eye.

tion is in the direction that reduces the disagreement with the data but is not large enough to bring about agreement. Increasing β from 0.25 to 0.30 increased $C_{j\alpha}$ only 10% for $l=0$ transitions. It is unrealistic to increase β enough to fit the experimental data.

Another possible explanation of the discrepancy is to attribute it to inadequate treatment of the tails of the bound-state wave functions, as Erskine¹ has suggested for reactions below the Coulomb barrier. To check whether this explanation holds also for reactions above the Coulomb barrier, proton spectra of the $^{235}\text{U}(d,p)^{236}\text{U}$ reaction leading to members of the $K^\pi = 3^-$ and 4^- bands were measured at bombarding energies of 14 and 16 MeV. The analysis of the data at these higher energies was the same as that for the 12-MeV data. For $E_d = 14$ and 16 MeV as well as 12 MeV, the single-particle cross sections ϕ_l extracted from the differential cross sections measured at 90° are shown in Fig. 7. The discrepancy between the experimental and calculated cross sections for the $\frac{1}{2}^+[631]$ orbital is seen to be of the same type at the higher bombarding energies as at 12 MeV:

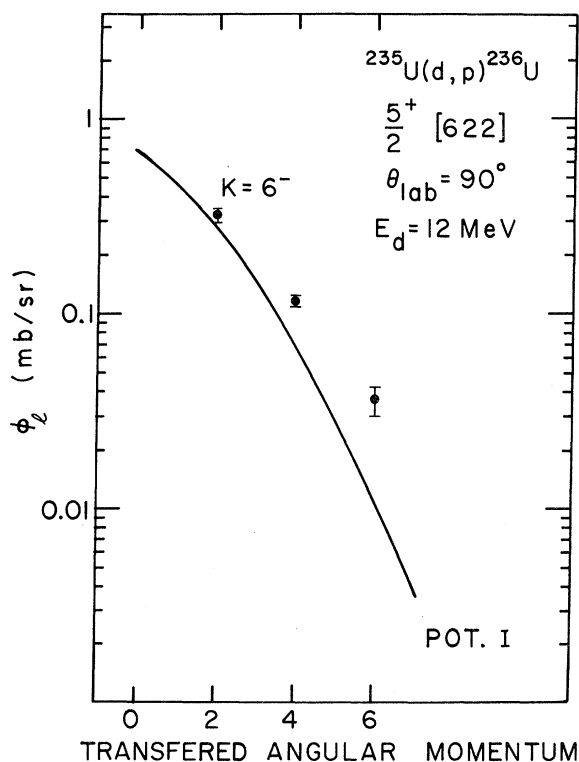


FIG. 8. Single-particle cross section ϕ_l extracted from the experimental cross sections for transitions to members in the $K^\pi = 6^-$ band. The single-particle cross section calculated with potential I is also plotted for comparison.

the $l=0$ component is diminished and the $l=4$ and $l=6$ components are enhanced.

In order to emphasize the energy dependence of the cross section, the ratio between the extracted and calculated cross sections at each bombarding energy was calculated for each transferred angular momentum. The averaged ratios for the $K^\pi = 3^-$ and 4^- bands are plotted in Fig. 9. Except for the $l=2$ transition at 12 MeV, the ratios for each transferred angular momentum are roughly constant. At all energies, the measured cross section for the $l=0$ component of the transition is only about half of the calculated value, and the measured cross section for $l=4$ is 2–3 times the calculated one. These energy-independent discrepancies may be due to an inadequate model of the bound-state wave function for the $\frac{1}{2}^+[631]$ orbital. However, the twofold increase in the cross section for the $l=2$ component at 12 MeV probably cannot be attributed to this cause; perhaps it indicates the importance of two-step processes²⁴ due to inelastic scattering in the incoming and/or outgoing channels at $E_d = 12$ MeV. Through the two-step processes, the destructive interference between Coulomb and nuclear excitation in the inelastic scattering channel²⁵ may be reflected on the cross section for the (d,p) reaction.

B. Moment of Inertia

The level energies in a rotational band are described to first order by the formula²⁶

$$E_x = A[I(I+1) - K^2] + E_0, \quad (4)$$

where the parameter A is related to the effective moment of inertia \mathcal{J}_0 through the expression $A = \hbar^2/2\mathcal{J}_0$. The A values extracted from the mea-

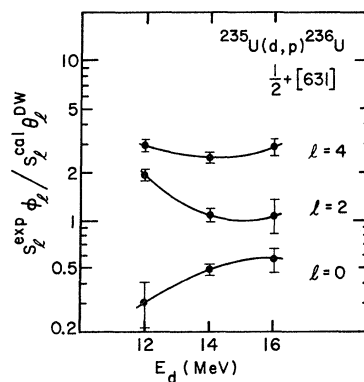


FIG. 9 The ratio $S_l^{\text{exp}} \phi_l / S_l^{\text{cal}} \theta_l^{\text{DW}}$, at several bombarding energies where $S_l \phi_l$ is the cross section for the transition to a state with orbital angular momentum l . The curves are hand drawn lines to connect the data points.

TABLE V. Summary of the values of the parameter $A = \hbar^2/2\mathcal{J}_0$ for two-quasiparticle states and for collective states in ^{236}U and ^{234}U . For ^{236}U the two-quasiparticle data are from the present work and the collective data are from Nuclear Data B4. For ^{234}U , all data are from Ref. 9, and the collective data are also reproduced in Nuclear Data B4.

Isotope	State	K	A (keV)
$^{236}_{92}\text{U}_{144}$	$\frac{7}{2}^- [743] + \frac{1}{2}^+ [631]$	3^-	5.05 ± 0.17
		4^-	5.02 ± 0.12
	$\frac{7}{2}^- [743] + \frac{5}{2}^+ [622]$	6^-	4.97 ± 0.17
		1^-	6.69 ± 0.34
	Ground state	0^+	7.11
	β vibration	0^+	7.32
	γ vibration	2^+	7.5
$^{234}_{92}\text{U}_{142}$	$\frac{5}{2}^+ [633] + \frac{1}{2}^+ [631]$	2^+	6.28 ± 0.24
		3^+	5.84 ± 0.15
	$\frac{7}{2}^- [743] + \frac{3}{2}^+ [631]$	2^-	5.73 ± 0.17
		5^-	4.50 ± 0.35
	$\frac{7}{2}^- [743] + \frac{5}{2}^+ [633]$	1^-	5.25 ± 0.15
		6^-	4.82 ± 0.19
	$\frac{7}{2}^- [743] + \frac{1}{2}^- [501]$	3^+	5.50 ± 1.12
		4^+	4.59 ± 0.41
	Ground state	0^+	7.26
	β vibration	0^+	6.93
	γ vibration	2^+	7.13

sured excitation energies of the rotational band built on two-quasiparticle states in ^{234}U and ^{236}U are summarized in Table V, together with A parameters for the ground-state band and for the β and γ vibrational bands. For the collective states, the A parameters have values near 7 keV. On the other hand, the A parameters for bands built on two-quasiparticle states average about 5 keV. This suggests that breaking up a pair and thereby producing two nucleons outside a core increases the moment of inertia by 40%. The average values of A in the neighboring odd-odd actinide nuclei are reported²⁰ to be 5 keV. This is consistent with the situation in the rare earth region, where the observed average values of A indicate that the moment of inertia is greater for the bands based on two-quasiparticle states than for the ground-state band.²⁷ It should be mentioned that the moments of inertia for the $K^\pi = 1^-$ band in ^{236}U and for the $K^\pi = 1^-, 2^-, 2^+, \text{ and } 3^+$ bands in ^{234}U deviate significantly from the average value $A = 5$ keV. In these cases, the deviation seems to be strongly correlated with the impurity in the two-quasiparticle component. The purity of this component (summarized in the last column of Table VI) can be obtained from an analysis of the cross sections to these bands.

C. Energy Splittings Between States with Parallel and Antiparallel Coupling

When two odd particles in a deformed nucleus are coupled outside a core, the projection of their spins on the intrinsic symmetry axis can combine only to give either $K_\gt = \Omega_1 + \Omega_2$ for parallel coupling

TABLE VI. Summary of energy splittings for two-quasiparticle states in even-even actinide nuclei. Data for ^{234}U are taken from Ref. 9. The fourth column shows the coupling of intrinsic spins for two-quasiparticles. No exception to the inverse Gallagher-Moszkowski rule is seen. The square of the amplitude (last column) is a measure of the purity of the two-quasiparticle component of the band.

Nuclide	$\Omega_1 [N_1 n_{z_1} l_1]$	+	$\Omega_2 [N_2 n_{z_2} l_2]$	Σ	K_f, I_f	E_x (keV)	ΔE^a (keV)	Purity (%)
$^{234}_{92}\text{U}_{142}$	$\frac{5}{2}^+ [633]$	+	$\frac{1}{2}^+ [631]$	1	3^+	1496	-369	100
				0	2^+	1127		30 ± 7
	$\frac{7}{2}^- [743]$	+	$\frac{3}{2}^+ [631]$	1	5^-	1693	-703	100
				0	2^-	990		58 ± 10
	$\frac{7}{2}^- [743]$	+	$\frac{5}{2}^+ [633]$	1	1^-	1434	13	100 ± 20
				0	6^-	1421		100
	$\frac{7}{2}^- [743]$	+	$\frac{1}{2}^- [501]$	1	3^+	1956	72	100
				0	4^+	1884		100
$^{236}_{92}\text{U}_{144}$	$\frac{7}{2}^- [743]$	+	$\frac{1}{2}^+ [631]$	1	3^-	1191.6	137.7	100
				0	4^-	1053.9		100
	$\frac{7}{2}^- [743]$	+	$\frac{5}{2}^+ [622]$	1	6^-	1471.7	-502.0	100
				0	1^-	969.7		74 ± 12

^a $\Delta E = E(K_\lt) - E(K_\gt)$.

or $K_< = |\Omega_1 - \Omega_2|$ for antiparallel coupling. The two resulting states are degenerate except as they are affected by residual interactions and Coriolis interactions. The formalism for calculating the energy splitting due to the effects of the residual interaction will be discussed in this section.

For odd-odd nuclei in the region of deformed rare earth nuclei, Jones *et al.*²⁸ have calculated the energy splittings in 20 pairs of states coupled parallel and antiparallel. They find that the experimental energy splittings can be well reproduced by a (zero-range) δ force and that the agreement is not improved by using a finite-range force with exchange character. However, a finite-range interaction and tensor force significantly improve the agreement between experiment and calculation in the odd-even shifts in $K^\pi = 0^-$ bands.

Anantaraman and Schiffer have analyzed²⁹ the splittings of multiplets in even-even and odd-odd spherical nuclei differing from doubly-closed shells by two nucleons. By using a large number of multiplets of levels from nuclei covering a wide range in mass and by searching the parameters of the residual interaction, they have determined a unique set of strengths and ranges for the effective residual interaction. In an earlier analysis of n - p states, Moinester, Schiffer, and Alford³⁰ found that a δ -function force with spin exchange seems to reproduce the data. However, Anantaraman and Schiffer, who included new data on $T=1$ matrix elements, find that the good δ -function fits are a fortuitous result of a cancellation between the finite-range attractive and repulsive parts of the effective interaction and that fits to the matrix elements with the $T=1$ component require a finite-range interaction with two ranges of 1.0 and 3.2 fm.

The energy splittings between states with parallel and antiparallel coupling of identical particles in even-even deformed nuclei have been calculated only for ¹⁶⁶Er. In these calculations with a zero-range force, Pyatov³¹ found a large discrepancy with experiment.

The residual interaction between *identical* particles ($T=1$) will be emphasized in the present work because this case is the simplest to study. In particular, the energy splittings between two-quasiparticle states in ²³⁴U and in ²³⁶U will be calculated both with zero-range and with finite-range forces.

The particular choice of effective residual two-body interaction will determine whether or not the removal of the degeneracy of a pair of two-quasiparticle states will result in a shift in the average energy as well as a splitting. Both the energy splitting and the energy shift should be fitted with the same strength and range parameters. For this

purpose, we have used the program KKSPLIT,³² in which the basic formulas are as follows. After the effect of Coriolis interactions is removed, the energies $K_>$ and $K_<$ of the states with parallel and antiparallel coupling, respectively, are given by

$$E(I, K_>) = (\hbar^2/2g_0)[I(I+1) - K_>^2] + E_{12} + \langle (\Omega_1 \Omega_2) IK_> | V_{\text{res}} | (\Omega_1 \Omega_2) IK_> \rangle_{QP}, \quad (5)$$

where $K_> = |\Omega_1 \pm \Omega_2|$ and E_{12} , the sum of the energies of the two degenerate quasiparticle states, is calculated by an exact pairing-force solution³³ of the known single-particle spectrum with levels 1 and 2 blocked. The matrix element in Eq. (5) will be explained in more detail in a paper by Weller.³² Since a band head has $I=K$, the energy shift from the energy of the degenerate-unperturbed two-quasiparticle states can be written as

$$E(K_>) - E_{12} = (\hbar^2/2g_0)K_> + \langle (\Omega_1 \Omega_2) IK_> | V_{\text{res}} | (\Omega_1 \Omega_2) IK_> \rangle_{QP},$$

and

$$E(K_<) - E_{12} = (\hbar^2/2g_0)K_< + \langle (\Omega_1 \Omega_2) IK_< | V_{\text{res}} | (\Omega_1 \Omega_2) IK_< \rangle_{QP}.$$

In a first-order approximation, the Nilsson wave functions can be used to represent the $|(\Omega_1 \Omega_2) IK_>|$ state, and the effective residual two-body interaction can be the same as is used for spherical nuclei. If we concern ourselves only with the energy splitting between states with $K_> = |\Omega_1 \pm \Omega_2|$, contributions that involve the pairing emptiness factors $(1 - U_\alpha^2)$ will cancel out³² in calculating the matrix element

$$\langle (\Omega_1, \Omega_2) IK_> | V_{\text{res}} | (\Omega_1, \Omega_2) IK_> \rangle_{QP}.$$

Thus the energy splitting between states with parallel and antiparallel coupling is simply given by

$$\begin{aligned} \Delta E &= E(K_<) - E(K_>) \\ &= (\hbar^2/2g_0)K_< - (\hbar^2/2g_0)K_> \\ &\quad + \langle IK_< | V_{12} | IK_< \rangle - \langle IK_> | V_{12} | IK_> \rangle. \end{aligned} \quad (6)$$

Here the effective residual two-body interaction is taken to be the conventional potential

$$V_{12}(|\mathfrak{F}_1 - \mathfrak{F}_2|) = f(|\mathfrak{F}_1 - \mathfrak{F}_2|) \times (WP^W + MP^M + BP^B + HP^H), \quad (7)$$

where W , M , B , and H are the strengths (in MeV) of the Wigner, Majorana, Bartlett, and Heisenberg potentials, respectively, P^W , P^M , P^B , and P^H are the corresponding exchange operators, $f(|\mathfrak{F}_1 - \mathfrak{F}_2|)$ is the radial form factor and is chosen to be either a δ function or a Gaussian of the form

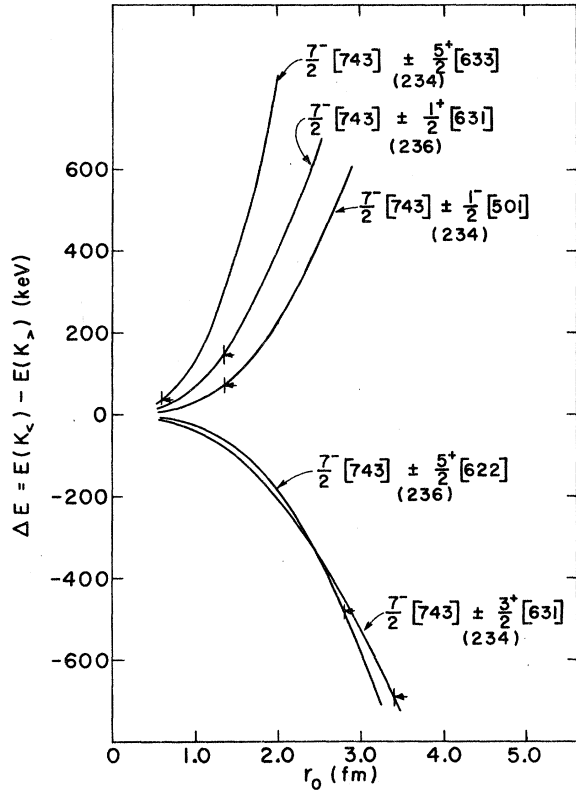


FIG. 10. Calculated energy splittings for the indicated configurations in ^{236}U (labeled 236) and ^{234}U (labeled 234), plotted as a function of the nuclear radius in the residual interaction. The Rosenfeld force with $V_0 = -100$ MeV is used in this case. For each curve, the vertical mark indicated by an arrow indicates the experimental value corrected by the rotational energy difference in the first part of Eq. (6).

$\exp(-r_{12}^2/r_0^2) \equiv \exp(-|\vec{r}_1 - \vec{r}_2|^2/r_0^2)$, and r_0 is the range parameter.

For identical particles ($T=1$), the matrix element of the Wigner potential is known to be equivalent to that of the Heisenberg potential with an opposite sign, and the matrix element of the Bartlett potential is also equal to that of the Majorana potential with an opposite sign for the same form factor. Therefore, the independent parameters are reduced to two potential strength parameters, $(W-H)$ and $(M-B)$, and one range parameter r_0 in this special case.

To illustrate how the residual two-body interaction affects the states with $K_{\pm} = |\Omega_1 \pm \Omega_2|$, we have calculated the energy splittings for five pairs of two-quasiparticle states in ^{234}U and ^{236}U . Measured energy splittings and band-head energies are listed in Table VI, along with the purities of two-quasiparticle states as obtained from the cross-section data. In these calculations, the Nilsson

wave functions used were those developed by Chi,³⁴ and the parameters were $\delta = 0.3$, $\mu = 0.448$, and $\kappa = 0.05$ for $N=6$ states and $\delta = 0.3$, $\mu = 0.434$, and $\kappa = 0.05$ for $N=7$ states; and we used a Rosenfeld mixture³⁵ of forces ($W/V_0 = 0.13$, $M/V_0 = -0.93$, $B/V_0 = -0.46$, and $H/V_0 = -0.26$, where $V_0 = W + M + B + H$). The strength parameter was held fixed at $V_0 = -100$ MeV, while the range parameter r_0 was left adjustable. The calculated energy splittings for this illustrative calculation are shown in Fig. 10. The arrows indicate the measured energy splittings for the states involved. The energy splittings for three of these pairs of states are reproduced by the calculation with a range $r_0 = 0.8-1.3$ fm, but the range for the $7/2^- [743] \pm 5/2^+ [622]$ and the $7/2^- [743] \pm 3/2^+ [631]$ pairs appears to be much larger. The large measured separations in the latter two pairs may indicate that the member with lower spin in each is not a pure two-quasiparticle state.

A zero-range interaction was also used to calculate the splittings of these five pairs. The extracted strengths did not converge to one value but scattered over the range from 37 to 4220 MeV.

We have also calculated the energy splittings with the two-range strength parameters, namely $(W-H)/(M-B) = -237.5$ MeV/22.5 MeV with $r_0 = 1.0$ fm and $(W-H)/(M-B) = 7.4$ MeV/0 MeV with $r_0 = 3.0$ fm, which were taken from the values that fit the data for spherical Pb nuclei.²⁹ The energy splittings can be described within 40 keV for the $7/2^- [743] \pm 1/2^+ [631]$ and the $7/2^- [743] \pm 1/2^- [501]$ states, but those of the other three pairs could not be reproduced.

The number of two-quasiparticle states observed in ^{234}U and ^{236}U was not large enough for a determination of a unique set of forms and strengths for the residual two-body interaction in deformed nuclei. When enough additional data of this type have been obtained and the calculated shifts of the energies of K_+ and K_- states from the unperturbed energies of these two-quasiparticle states are included, one should be able to decide on the most suitable description of the residual interactions in deformed heavy nuclei. Such calculations on data from both the present work on ^{234}U and ^{236}U and a similar study on ^{248}Cf and ^{250}Cf will be reported in a forthcoming paper, in which the observed energies of a total of twelve pairs of $n-n$ states with $T=1$ components will be used to test the calculations made with a series of potentials.

From our experimental results for two-quasiparticle states we can make some comments on the rule for coupling the angular momenta of individual-particle states in even-even deformed nuclei. It is well known that the Gallagher-Moszkowski rule³⁶ is widely applicable in odd-odd deformed nuclei.

For nonidentical particles (e.g., for n - p states), the rule predicts that the state with parallel intrinsic spins ($\Sigma = 1$) has a lower energy than the state with antiparallel intrinsic spins ($\Sigma = 0$). In the even-even nuclei, in which two identical particles (two neutrons or two protons) combine, the reverse level order is anticipated.³⁷ As can be seen in Table VI, we have evidence supporting the inverse Gallagher-Moszkowski rule which predicts that the state with $\Sigma = 0$ should be below the one with $\Sigma = 1$.

VI. SUMMARY

Two-quasiparticle states in the even-even nucleus ^{236}U are selectively excited through the (d, p) reaction on ^{235}U . Four bands with $K^\pi = 3^-, 4^-, 1^-,$ and 6^- have been identified by three independent methods. The purity of these two-quasiparticle states has been obtained from the double ratios $\bar{R}/\bar{R}_{\text{pure}}$ between the ratio \bar{R} of the measured-summed cross section in the band to the calculated cross section and the corresponding ratio \bar{R}_{pure} for the band based on a pure two-quasiparticle state. This method of extracting the purity P of the band is relatively little affected by ambiguities in the DWBA calculation or by pairing. Therefore the resulting value of P (also called "the square of the amplitude") is of special importance. The purity of the band can also be estimated from the amounts by which the state $K_- = |\Omega_1 - \Omega_2|$ is shifted away from the state $K_+ = \Omega_1 + \Omega_2$. Further evidence on the degree of purity comes from the moments of inertia found for the different bands.

At bombarding energies from 12 to 16 MeV, the

cross sections calculated with Nilsson wave functions in the conventional DW formalism tend to be 2–3 times the measured cross sections for $l=0$ transitions; but for $l=4$ and 6 transitions, the calculated cross sections are smaller than the measured ones by a factor of 2–6. This discrepancy between the calculated and measured single-particle cross sections may arise mainly from improper treatment of the tails of bound-state wave functions and from the neglect of two-step processes.

The forms and magnitudes of the effective residual two-body interactions for identical particles in the strongly deformed nuclei were investigated by calculating their effect on the energy splittings between states with parallel and antiparallel coupling, but the number of two-quasiparticle states available was not great enough to determine the interaction parameters uniquely. The effect of the residual two-body interaction was illustrated by a calculation for five pairs of states observed in ^{234}U and ^{236}U .

ACKNOWLEDGMENTS

We are deeply indebted to Dr. J. P. Schiffer and Dr. D. Kurath for helpful discussions and comments throughout this work. We also thank Dr. F. Weller for many useful comments and for supplying the computer code KKSPLIT used in the calculation of the energy splittings. We are grateful to Dr. J. S. Boyno for sending data before publication. We are indebted to J. R. Lerner for preparing the ^{235}U target with an isotope mass separator.

*Work performed under the auspices of the U.S. Atomic Energy Commission.

†On leave from Tokyo University of Education, Tokyo, Japan.

¹J. R. Erskine, Phys. Rev. C **5**, 959 (1972).

²T. H. Braid, R. R. Chasman, J. R. Erskine, and A. M. Friedman, Phys. Rev. C **1**, 275 (1970).

³T. von Egidy, Th. W. Elze, and J. R. Huizenga, Nucl. Phys **A145**, 306 (1970); J. S. Boyno, Th. W. Elze, and J. R. Huizenga, *ibid.* **A157**, 263 (1970).

⁴F. A. Rickey, E. T. Jurney, and H. C. Britt, Phys. Rev. C **5**, 2072 (1972).

⁵W. R. Kane, Phys. Rev. Lett. **25**, 953 (1970).

⁶B. Fogelberg and A. Bäcklin, in *Contributions, Conference on Nuclear Structure Study with Neutrons, Budapest, Hungary, 1972* (Central Research Institute for Physics, Budapest, 1972), p. 6.

⁷J. V. Maher, J. R. Erskine, A. M. Friedman, R. H. Siemssen, and J. P. Schiffer, Phys. Rev. C **5**, 1380 (1972).

⁸J. S. Boyno, Th. W. Elze, J. R. Huizenga, and O. E. Bemis, Jr., Bull. Am. Phys. Soc. **17**, 463 (1972).

⁹S. Bjornholm, J. Dubois, and B. Elbek, Nucl. Phys. **A118**, 241 (1968).

¹⁰J. E. Spencer and H. A. Enge, Nucl. Instrum. Methods **49**, 181 (1967).

¹¹J. R. Erskine and R. H. Vonderohe, Nucl. Instrum. Methods **81**, 221 (1970).

¹²N. Williams, private communication.

¹³P. Spink and J. R. Erskine, Argonne National Laboratory Physics Division Informal Report No. PHY-1965B (unpublished); J. R. Comfort, Argonne National Laboratory Physics Division Informal Report No. PHY-1970B (unpublished).

¹⁴G. R. Stachler, Ann. Phys. (N.Y.) **3**, 275 (1958); S. G. Nilsson, K. Dan. Vidensk. Selsk., Mat.-Fys. Medd. **29**, No. 16 (1955).

¹⁵We are grateful to Dr. P. D. Kunz for making this code available to us.

¹⁶B. E. F. Macefield and R. Middleton, Nucl. Phys. **59**, 561 (1964).

¹⁷F. D. Becchetti, Jr., and G. W. Greenlees, John H. Williams Laboratory of Nuclear Physics, University of Minnesota, Annual Report, 1969 (unpublished),

- p. 116.
- ¹⁸J. R. Erskine and W. W. Buechner, *Phys. Rev.* **133**, B370 (1964).
- ¹⁹C. M. Lederer, J. M. Hollander, and I. Perlman, *Table of Isotopes* (Wiley, New York, 1968), 6th ed.
- ²⁰K. Katori and A. M. Friedman, *Bull. Am. Phys. Soc.* **17**, 463 (1972).
- ²¹Th. W. Elze and J. R. Huizenga, *Nucl. Phys.* **A187**, 545 (1972).
- ²²C. M. Lederer, J. M. Jaklevic, and S. G. Prussin, *Nucl. Phys.* **A135**, 36 (1969).
- ²³A. J. Ferguson, *Angular Correlation Methods in Gamma-Ray Spectroscopy* (North-Holland, Amsterdam, 1965), p. 104.
- ²⁴N. K. Glendenning and R. S. Mackintosh, *Nucl. Phys.* **A168**, 575 (1971).
- ²⁵For a typical example, see F. Videbaek, I. Chernov, P. R. Christensen, and E. E. Gross, *Phys. Rev. Lett.* **28**, 1072 (1972).
- ²⁶J. P. Davidson, *Collective Models of the Nucleus* (Academic, New York, 1968), p. 83.
- ²⁷J. I. Zaitz and R. K. Sheline, *Phys. Rev. C* **6**, 506 (1972); D. G. Burke and B. Elbek, *K. Dan. Vidensk. Selsk. Mat.-Fys. Skr.* **36**, No. 6 (1967); R. A. Harlan and R. K. Sheline, *Phys. Rev.* **160**, 1005 (1967); A. Bäcklin, A. Suarez, O. W. B. Schult, B. P. K. Maier, U. Gruber, E. B. Shera, D. W. Hafemeister, W. N. Shelton, and R. K. Sheline, *Phys. Rev.* **160**, 1011 (1967).
- ²⁸H. D. Jones, N. Ohnishi, T. Hess, and R. K. Sheline, *Phys. Rev. C* **3**, 529 (1971).
- ²⁹N. Anantaraman and J. P. Schiffer, *Phys. Lett.* **37B**, 229 (1971).
- ³⁰M. Moinester, J. P. Schiffer, and W. P. Alford, *Phys. Rev.* **179**, 984 (1969).
- ³¹N. I. Pyatov, *Izv. Akad. Nauk SSSR Ser. Fiz.* **27**, 1436 (1963) [transl.: *Bull. Acad. Sci. USSR Phys. Ser.* **27**, 1409 (1963)].
- ³²K. Katori and F. Weller, *Bull. Am. Phys. Soc.* **17**, 674 (1972); F. Weller, to be published.
- ³³R. R. Chasman, private communication.
- ³⁴B. H. Chi, *Nucl. Phys.* **83**, 97 (1966).
- ³⁵L. Rosenfeld, *Nuclear Forces* (North-Holland, Amsterdam, 1948), p. 233.
- ³⁶C. J. Gallagher and S. A. Moszkowski, *Phys. Rev.* **111**, 1282 (1958).
- ³⁷C. J. Gallagher and V. G. Soloviev, *K. Dan. Vidensk. Selsk. Mat.-Fys. Skr.* **2**, No. 2 (1962).